HERMES Results on the Spin Structure of the Nucleon

Pasquale Di Nezza
INFN, Laboratori Nazionali di Frascati, Italy
On behalf of the HERMES Collaboration

Abstract

The HERMES experiment at HERA is studying the spin structure of the nucleon. By using polarised internal gas targets and a large acceptance forward spectrometer, HERMES performs accurate measurements of inclusive and semi-inclusive deep inelastic scattering processes. In this talk the main results on $g_1^{p,n}(x)$ structure functions, polarized quark distributions, sum rules, azimuthal hadron distributions, fragmentation functions, pseudoscalar- and vector-meson electroproduction are presented.

1 Introduction

Deep inelastic lepton-nucleon scattering (DIS) plays an essential role in the development of present understanding of the sub-structure of hadrons. The DIS differential cross section in the one-photon exchange approximation can be written as [1]:

$$\frac{d^3\sigma}{dx dy d\phi} = \frac{\alpha^2}{Q^4}\frac{y}{2}L_{\mu\nu}W^{\mu\nu}, \tag{1}$$

where $L_{\mu\nu}$ and $W^{\mu\nu}$ involve the leptonic and hadronic electromagnetic currents respectively. The former is well known from QED, while the latter contains the non-perturbative structure of the nucleon. For a spin-$\frac{1}{2}$ target, it can be expressed by two unpolarised, F_1 and F_2, and two polarised , g_1 and g_2, structure functions, each of them can be isolated and measured with appropriate choices of the kinematics and of the beam and target polarisations.

Defining $q_i^{+(-)}(x)$ as the sum of quark distributions with flavour i and spin parallel (antiparallel) to the nucleon spin, in the Quark Parton Model, for a longitudinally polarised target, the structure functions of the nucleons are given by:

$$F_1(x) = \frac{1}{2}\sum_{i=1}^{n} e_i^2 (q_i^+(x) + q_i^-(x)), \tag{2}$$

$$g_1(x) = \frac{1}{2}\sum_{i=1}^{n} e_i^2 (q_i^+(x) - q_i^-(x)) = \frac{1}{2}\sum_{i=1}^{n} e_i^2 \Delta q_i(x). \tag{3}$$

Therefore F_1 and g_1 represent the quark momentum and spin distributions in the nucleon and scale with the fraction x of the momentum of the parent nucleon. In the QCD frame, where the strong interactions among partons are considered, $g_1(x)$ is also Q^2-dependent and includes the gluon distribution function $\Delta g(y,Q^2)$, the singlet $\Delta\Sigma(y,Q^2)$ and the non-singlet combinations $\Delta q^{NS}(y,Q^2)$ of the quark distribution functions:

$$\begin{aligned} g_1(x,Q^2) &= \frac{1}{2}\sum_{i=1}^{n_f}\frac{e_i^2}{n_f}\int_x^1 \frac{dy}{y}[C_q^S(\frac{x}{y},\alpha_s(Q^2))\Delta\Sigma(y,Q^2) \\ &+ 2n_f C_g(\frac{x}{y},\alpha_s(Q^2))\Delta g(y,Q^2) \\ &+ C_q^{NS}(\frac{x}{y},\alpha_s(Q^2))\Delta q^{NS}(y,Q^2)], \end{aligned} \tag{4}$$

where C_q^{NS}, C_q^S and C_g are the coefficient functions which are calculable in perturbative QCD.

The integral of $g_1(x)$ over x (first momentum) represents the overall polarisation contribution of the quarks in the nucleon. Using the isospin invariance for the different quarks u,d,s ($\Delta u_p = \Delta d_n = \Delta u, \Delta d_p = \Delta u_n = \Delta d, \Delta s_p = \Delta s_n = \Delta s$) it is possible to formulate the QCD fundamental *Bjorken Sum Rule* assuming only the SU(2) symmetry [2]:

$$\int_0^1 [g_1^p(x) - g_1^n(x)]dx = \frac{1}{6}(\Delta u - \Delta d) = \frac{1}{6}\left|\frac{g_A}{g_V}\right| + QCD\ corrections, \tag{5}$$

where g_A and g_V are the axial and vector coupling constants measured in the neutron $\beta - decay$. Making further assumptions as $SU(3)_F$ symmetry and $\Delta s = 0$, Ellis and Jaffe derived additional sum rules [3] which relate the first momenta $\int_0^1 g_1^p(x)dx$ and $\int_0^1 g_1^n(x)dx$ to the F and D constants measured in neutron and hyperon $\beta - decays$.

The polarised structure function $g_1(x)$ is measured from the yields of scattering of longitudinally polarised leptons on longitudinally polarised nucleons. To get experimental access to $g_1(x)$ it is necessary to write a lepton asymmetries in terms of the virtual photon asymmetries $A_1(x,Q^2)$ and $A_2(x,Q^2)$. Neglecting the small contribution of $A_2(x,Q^2)$ one obtains:

$$g_1(x,Q^2) \approx F_1(x,Q^2)A_1(x). \tag{6}$$

With inclusive DIS it is not possible to separate the single flavour contributions to the total spin carried by the nucleon, because there are only two independent measurements on the neutron and the proton target. In semi-inclusive measurement a final state hadron is also detected in coincidence with the scattered lepton (see fig.1). By detecting and identifying the produced hadron, it suffices to measure the asymmetry $A_1^h(x,z)$ in the particle yields to determine the probability that a quark of flavour q is struck in that event (what is called *hadron purity* $P_q^h(x,z)$) to determine the polarised and non-polarised quark distribution function [4]:

$$A_1^h(x,z) \simeq \frac{1}{D}\frac{N_{\uparrow\downarrow}^h - N_{\uparrow\uparrow}^h}{N_{\uparrow\downarrow}^h + N_{\uparrow\uparrow}^h} = \sum_q P_q^h(x,z)\cdot\frac{\Delta q(x)}{q(x)}. \tag{7}$$

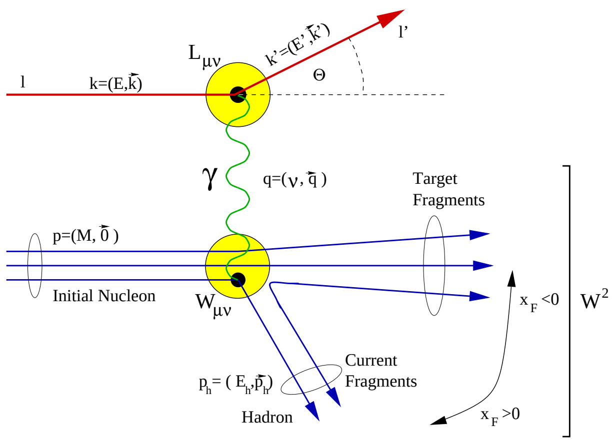

Figure 1: Diagram of the Semi Inclusive Deep Inelastic Scattering.

In this way it is possible to separate the single flavour contribution to the nucleon spin; the latter can be written as the sum of contributions from quarks, gluons and angular momenta:

$$\frac{1}{2} = \frac{1}{2}\Delta\Sigma + \Delta G + \Delta L, \tag{8}$$

where $\Delta\Sigma = \Delta u + \Delta d + \Delta s$. Combining all the experimental data now available, the current values are $\Delta\Sigma = 0.27 \pm 0.04$, $\Delta u = 0.82 \pm 0.03$, $\Delta d = -0.44 \pm 0.03$, $\Delta s = -0.11 \pm 0.03$, and nothing is known about ΔG or ΔL.

2 The HERMES experiment

HERMES has been designed to address many of the open questions concerning the spin structure of the nucleon using new experimental techniques to measure polarised DIS processes.

The HERMES experiment [5] is installed in the positron-proton collider HERA at DESY and uses the 27.5 GeV positron beam which is longitudinally polarised in the HERMES target region. In fig.2 is shown the beam polarisation fill measured by two Compton back-scattering polarimeters. HERMES is a forward spectrometer (see fig.4) with a dipole magnet providing an integrated field of 1.3 Tm. The magnet is divided into two identical sections by a horizontal iron plane that shields the positron and proton beams from the magnetic field. Consequently, the spectrometer consists of two identical detector systems, upper and lower, with a minimum polar angle for the acceptance of particles produced from the target region of 40 mrad. The maximum angular acceptances are ± 140 mrad vertically and ± 170 mrad horizontally. For particles with momenta from 4.5 to 27 GeV, the average momentum resolution $\Delta p/p$ is $0.7 - 1.3\%$. Particle identification (PID) is accomplished using a lead glass calorimeter, a scintillator hodoscope preceded by two radiation length of lead, a six-module transition detector and a $C_4F_{10}/N_2(70:30)$ gas threshold Čerenkov counter. A likelihood method provides clean positron-hadron separation

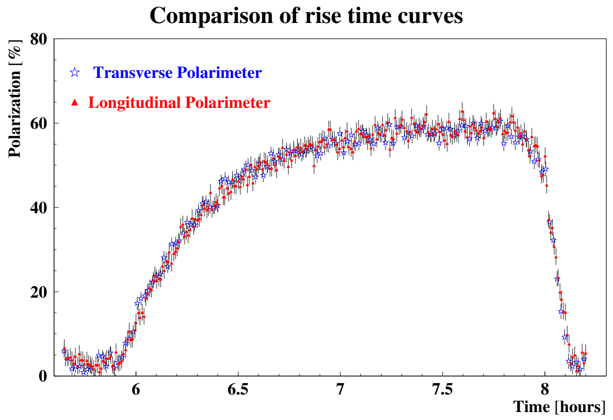

Figure 2: HERA positron beam polarisation for a short fill. It is shown the comparison between transverse and longitudinal measurements.

with an efficiency $> 98\%$ and a contamination $< 1\%$. The kinematical range accessible is wide with $0.02 < x < 0.8$ and $0.2 < Q^2 < 20\ GeV^2$.

Gas targets with high nuclear polarization and no dilution by unpolarised nucleons are used. The target cell, 40 cm long, is placed inside the positron storage ring. In 1995, the HERMES commissioning year, a ^3He polarised gas target, was used with an average polarisation of $(46 \pm 5)\%$ and an areal density of $10^{15}\ nucleon/cm^2$. To reduce systematic bias on spin dependent measurements, the target polarisation was reversed every 10 minutes. In 1996 and 1997 data were taken using a polarised hydrogen target with a polarisation of $(86 \pm 5)\%$ and a density of $7 \cdot 10^{13}\ nucleon/cm^2$; here, the target polarisation was reversed every minute (see fig.3). The luminosity in the range of $2 \div 30 \times 10^{31}\ nucleons \cdot cm^{-2} \cdot sec^{-1}$ is measured by the Bhabha scattering.

3 Inclusive Measurements

Fig.5 shows the $A_1^n(x)$ asymmetry and the $g_1^n(x, Q^2)$ structure function measured by HERMES [6] and the comparison with the dedicated E-154 experiment [7]. The larger statistical errors for HERMES is justified by the fact this measurement was done during the 1995 commission year. New data for the neutron will be produced in the 1998-2000 running period by using a deuterium target.

The $g_1^p(x, Q^2)$ structure function as measured in 1997 is plotted in fig.6 [10]. The measurement is compared with the E-143 one at $Q^2 = 2\ GeV^2$ and with the SMC one at $Q^2 = 10\ GeV^2$ [7][9]; the agreement between the experiments is good and the HERMES data have smaller errors. The statistical accuracy of the HERMES data will be further improved with the inclusion of the 1996 proton data.

Despite of the high precision reached by these measurements the interpretation of the data is still not conclusive. The limited x range doesn't allow an exact determination of the first moment of g_1, which is the only quantity that can be calculated by perturbative QCD. Using reliable theoretical models to extrapolate the measurements in the low-x range not covered by the experiments, is possible

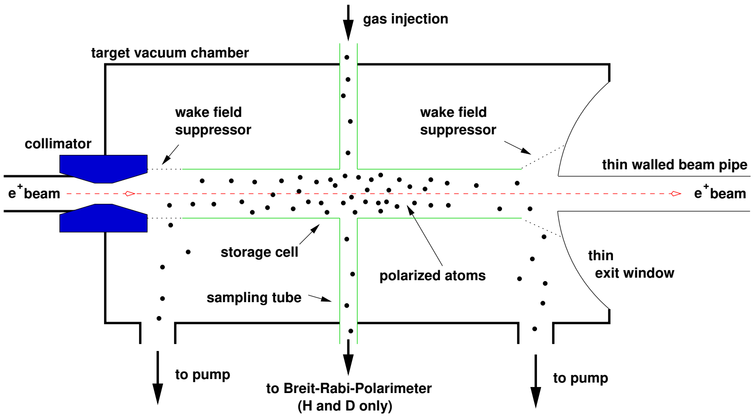

Figure 3: Target vacuum chamber scheme.

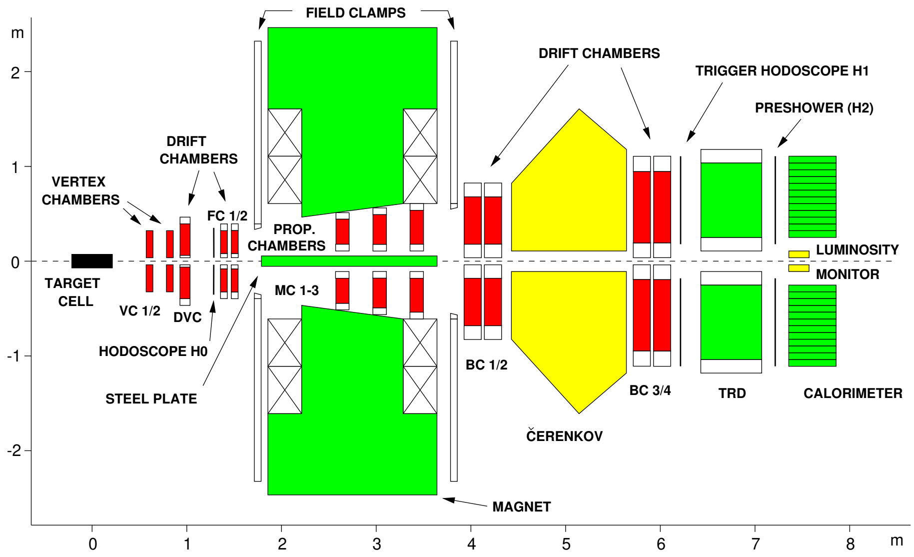

Figure 4: Longitudinal view of the HERMES spectrometer.

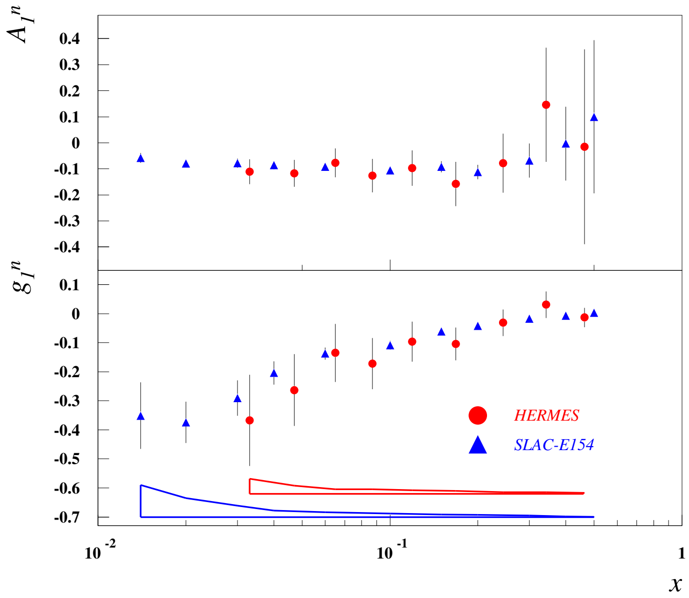

Figure 5: The HERMES neutron asymmetry $A_1^n(x)$ and spin structure function $g_1^n(x)$ compared to E154. The error bars are statistical uncertainties and the bands show the systematic errors.

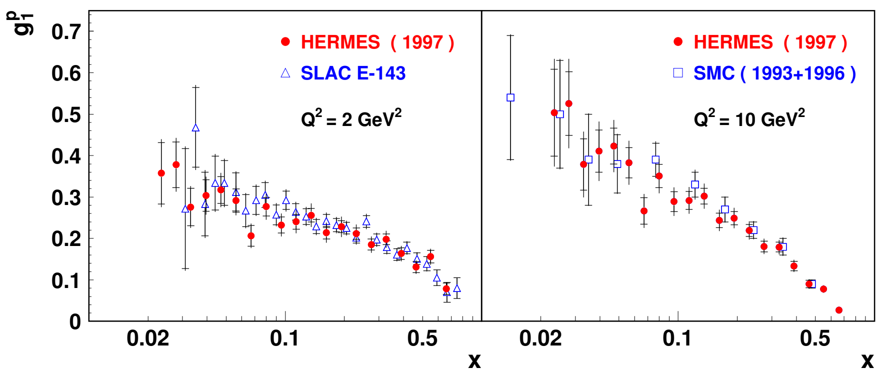

Figure 6: The HERMES proton structure function $g_1^p(x)$ compared with the E-143 experiment at $Q^2 = 2\ GeV^2$ and with SMC at $Q^2 = 10\ GeV^2$.

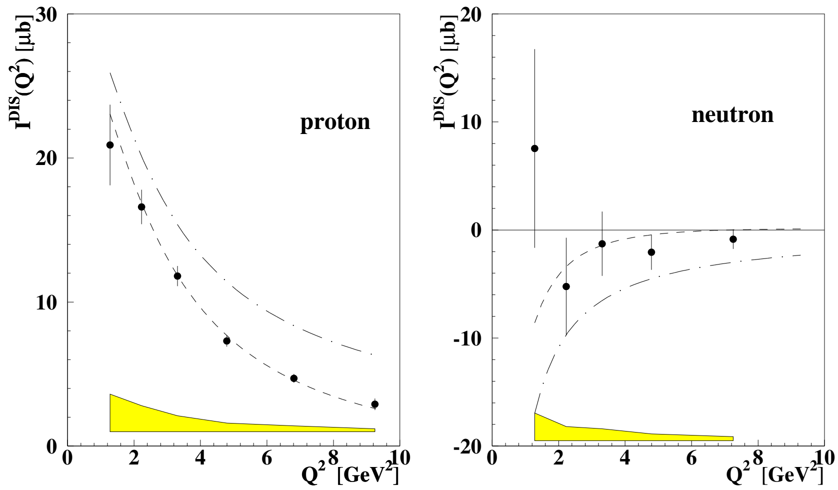

(a) (b)

Figure 7: The generalised GDH integral as function of Q^2 in the DIS region for proton and neutron.

to establish that the Bjorken sum rule is confirmed at 10% level while the Ellis-Jaffe sum rule is violated. This is an indication the strange sea quarks gives a spin contribution different from zero.

A relevant additional result in inclusive measurements obtained by HERMES is the first determination of the DIS contribution to the generalised GDH sum rule. This rule relates the anomalous contribution to the magnetic moment of the nucleon with the total absorption cross section for polarised real photons on polarised nucleons. Fig.7 shows, for both proton and neutron, the value of the generalised relevant integrals [11]. The dashed lines represent the integrals of a NLO parameterisation over the x range measured at HERMES for proton and neutron. The dash-dotted curves show the previous integrals including the low x contributions. For Q^2 above 1 GeV^2 the results are at least of the same order of magnitude as expectations for the resonance part of the generalised GDH integral.

4 Semi-Inclusive Measurements

In order to calculate the spin contribution from the single flavour, one needs to measure the A_1^h hadron asymmetry. In fig.8 results for the semi-inclusive asymmetries are shown for both hadrons and pions. The top rows present the results from the hydrogen and the bottom rows for the ^3He target. The limits $x_F > 0.1$ and $z > 0.2$ (for H), $z > 0.1$ (for ^3He) have been applied to suppress hadrons from the target region and to identify only the leading particles. In fig.9 are presented the HERMES results on the polarised quark distribution function. They have been derived, using the CTEQ parameterisation at low Q^2 for the unpolarised parton density functions and the measured fragmentation functions.

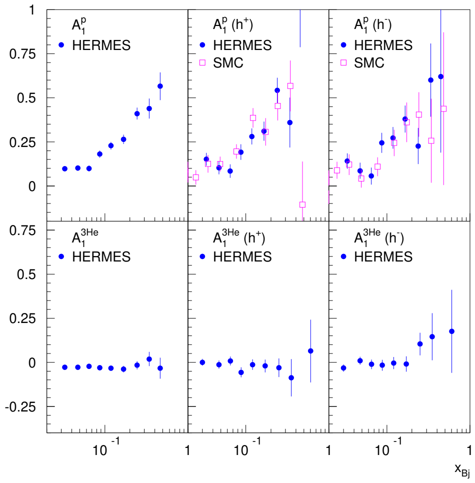

(a)

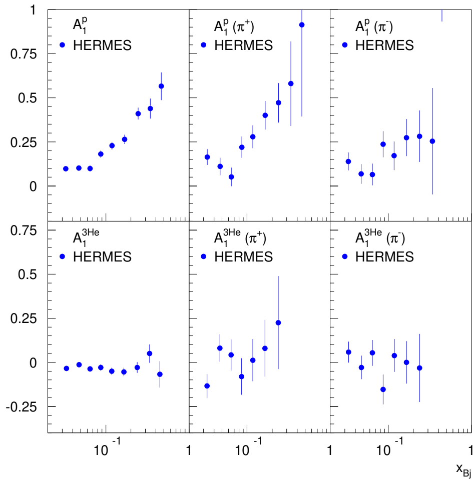

(b)

Figure 8: Hadron (a) and pion (b) asymmetries on the proton (top) and ${}^3He$ (bottom) compared to the inclusive ones and the SMC data for the hadron asymmetry.

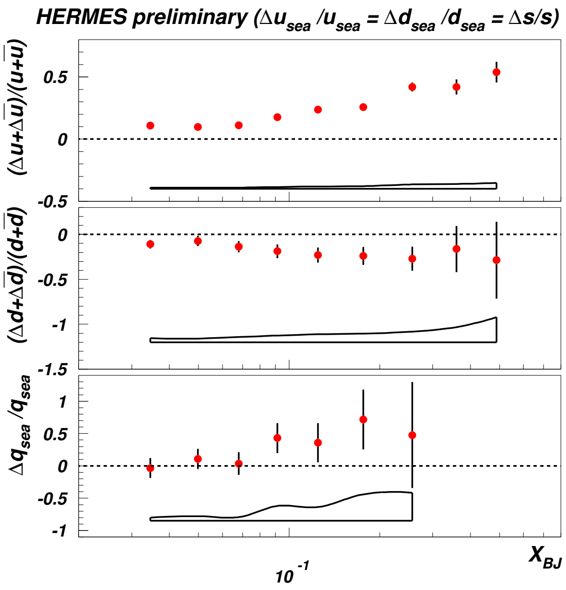

Figure 9: The flavour decomposition of the quark polarisation as function of x derived from the inclusive and semi-inclusive asymmetries. The sea polarisation is assumed to be flavour symmetric.

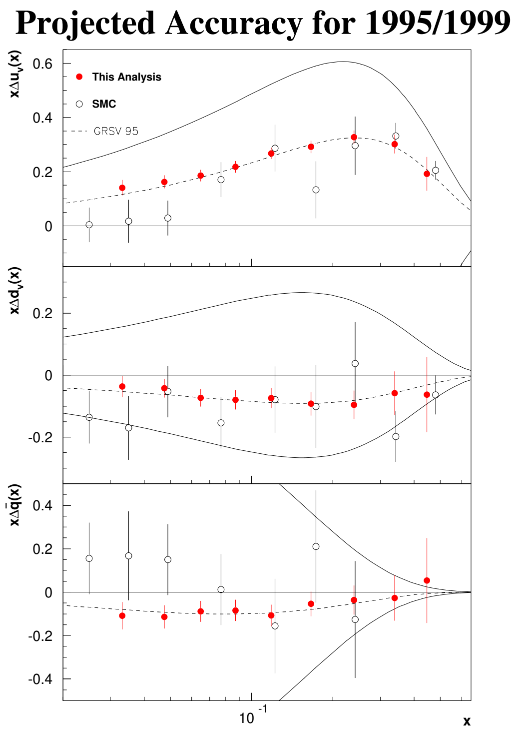

Figure 10: Projection of the expected polarised quark distribution function including all the data 1995-1999.

For all values of x the polarised distribution for the *up* (*down*) quark is positive (negative). Their absolute values are largest at large x and remain different from zero in the sea region. Taking the statistical and the systematic errors into account the sea quark distribution is compatible with zero over the measured range of x. The projection of the expected final HERMES statistical errors including all the data which will be collected within 1995-2000 is shown in fig.10. The projection is performed using the LO-GRSV parameterisation and the solid lines are the positivity limits.

Another important result of HERMES is the first measurement of the single-spin asymmetries in pion production in the distribution in azimuthal angle ϕ of the pion relative to the lepton scattering plane. A significant target spin asymmetry, fig.11, was observed in the $sin\phi$ moment of the cross section for positron scattering. This results can be interpreted as an effect of the "time-reversal-odd" fragmentation function arising from the non-perturbative hadronic final-state interactions [13].

5 Unpolarised Measurements

HERMES has also performed several measurements using unpolarised targets. Because of the flavour blindness of QCD the light quark sea should be symmetric. This assumption was questioned by the violation of the Gottfried sum rule, based on the

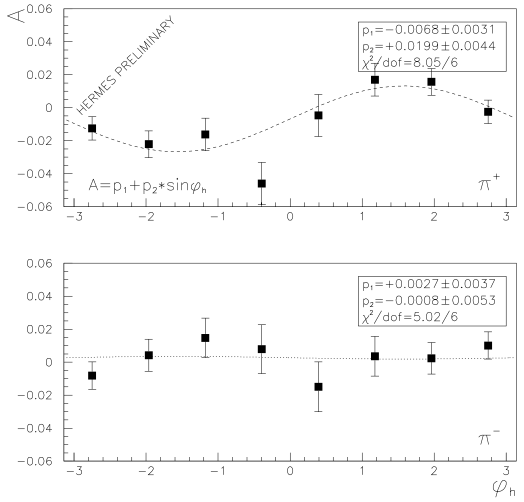

Figure 11: Spin azimuthal asymmetry in the π^+ and π^- cross sections.

isospin symmetry, observed by NMC [14]. The fig.12 shows the results, as a function of x, of the flavour asymmetry of the light sea by the flavour tagging method in semi-inclusive DIS obtained from a combination of charged pion yields. There, the HERMES results, are compared with the Drell-Yan data from E866 [15][16]. There is a large significant excess of $\bar{d}$ over $\bar{u}$ at low x. The two experiments give consistent values for $\bar{d} - \bar{u}$ even though the average Q^2 differs by about a factor of 20.

Other important results achieved by HERMES in the unpolarised electroproduction are in the diffractive, exclusively produced $\rho^0(770) \rightarrow \pi^+\pi^-$ mesons: here the analysis of the decay angular distribution can be used to study the spin-dependent properties of the production process. The polarisation of this meson changes rapidly with Q^2, it is transverse in the limit $Q^2 = 0$, but it becomes more and more longitudinal with increasing Q^2. As a consequence, as shown in fig.13, the angular distributions of the HERMES ρ^0 data change at different Q^2 values. The angles θ and ϕ are defined as the polar and the azimuthal angle of the π^+ in the ρ^0 center of mass system and ψ is the polarisation angle.

Moreover, using the incoherent exclusive ρ^0 production data from different targets as ^1H, ^2H, ^3He or ^{14}N, the nuclear transparency (T_A) has been studied as a function of the coherence length (l_c) of quark-antiquark fluctuation of the virtual photon [17]. As shown in fig.14(a), the nitrogen transparency, fig.14(b), exhibits the decrease expected from the onset of hadronic initial state interactions (ISI) as l_c increases. The decrease from 0.681 ± 0.060 at $l_c < 2\ fm$ to 0.401 ± 0.054 at $l_c > 3.6\ fm$ has 3.5 standard deviation statistical significance. In the absence of ISI variations, the transparency would exhibit a small ($< 3\%$) increase with l_c due to the known energy dependence of the $\rho^0 N$ cross section.

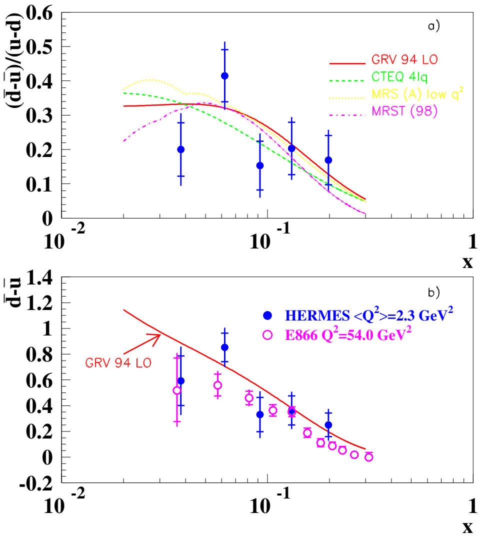

Figure 12: The light quark sea asymmetry compared to different models and to E866 experiment.

6 Outlook

In the 1998-2000 HERMES is mainly using a deuterium target to measure the $g_1^D(x)$ and to improve the $g_1^n(x)$ measurement made in the commissioning year with a ^3He target.

Since June 1998 HERMES has several detector upgrades in work to improve the performance of the spectrometer in the semi-inclusive measurements. A forward quadrupole spectrometer was installed downstream the experiment to detect electrons at very low Q^2. A test station of arrays of silicon-strip detector is located inside the target chamber; it will detect slow recoil protons to improve the J/Ψ reconstruction and to tag e-n events in e-D scattering. A second array of silicon strips in front of the target will allow to reconstruct short track and improve the Λ identification. A dual radiator, C_4F_{10} gas and *aerogel*, Ring Image Čerenkov detector (RICH) replaced the threshold gas Čerenkov counter to allow a clean detection of pions and kaons in the whole range $2-20\ GeV$. As a consequence the hadron fragmentation functions can be measured with high accuracy in order to reduce the systematic uncertainties in the Δq analysis. Furthermore the improving of the kaon detection allows HERMES to make the first semi-inclusive measurement of the strange quarks polarisation (Δs) as a function of x. In fig.15 is plotted the kaon asymmetry expected under the realistic hypothesis of 100 pb^{-1} of integrated luminosity collected in the 1999-2000. Finally, a muon filter (consisting of an iron wall plus an hodoscope) has been installed to increase the charm quark sensitivity, by the detection of the J/Ψ meson.

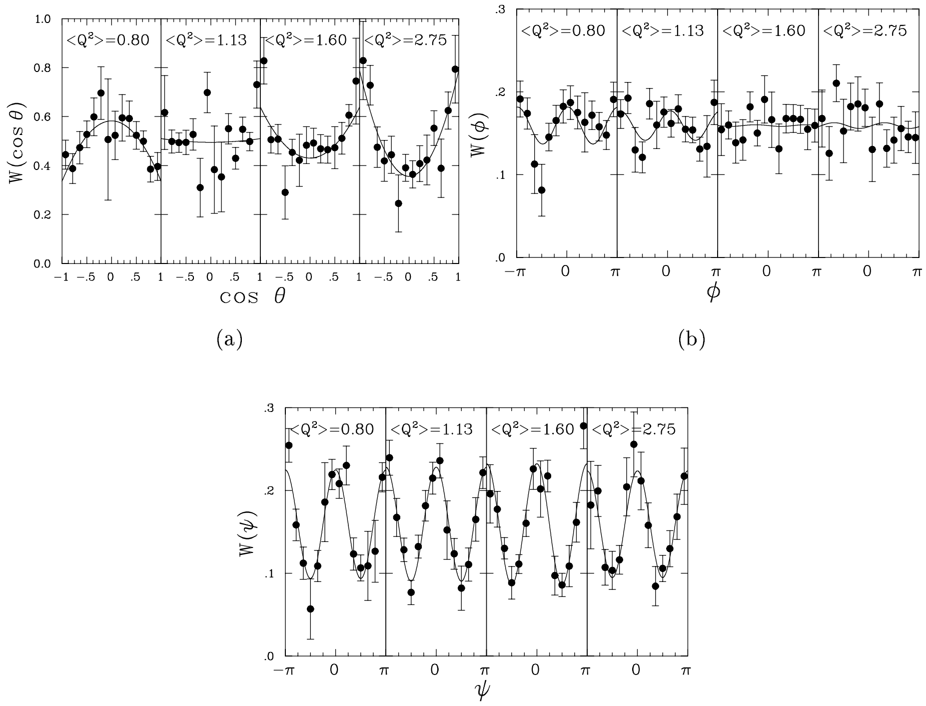

(a) (b)

(c)

Figure 13: Decay (a), azimuthal (b) and polarisation (c) angles of ρ^0 mesons produced in diffractive, exclusive electro-production.

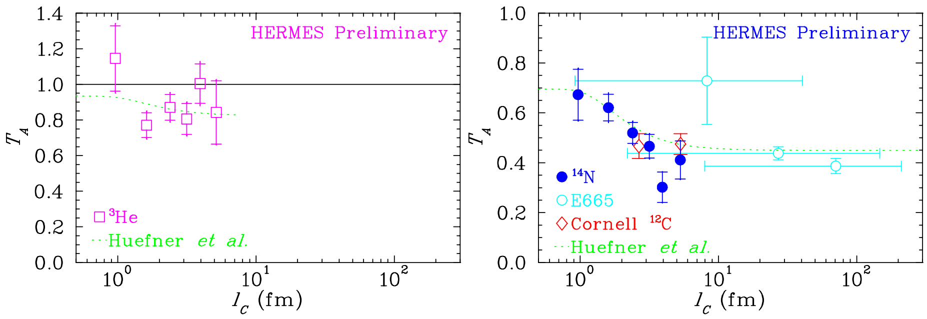

(a) (b)

Figure 14: Nuclear transparency T_A as a function of l_c. (b) includes comparison with previous experiments with photon (open diamond) and muons (open circle) beams. The dashed curves are the calculations for ^3He and ^{14}N targets.

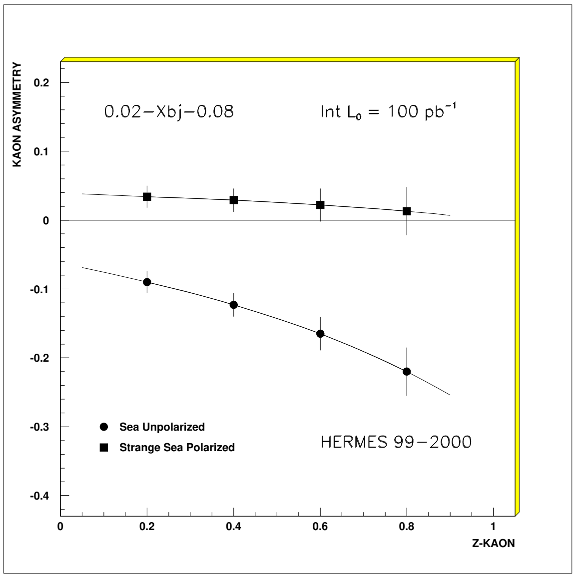

Figure 15: Expected kaon asymmetry for different sea quark polarisation values.

References

[1] R.G.Roberts, *The structure of the proton*, Cambridge University Press (1990)

[2] J.D.Bjorken, Phys.Rev. 148 (1996) 1467, Phys.Rev. D1 (1970) 1376

[3] J.Ellis and R.L.Jaffe, Phys.Rev. D9 (1974) 1444, Phys.Rev. D10 (1974) 1669

[4] D. de Florian et al., Nucl.Phys. B470 (1996) 195

[5] HERMES Collaboration, K.Ackerstaff et al., NIM A417 (1998) 230

[6] HERMES Collaboration, K.Akerstaff et al., Phys.Lett. B404 (1997) 383

[7] E154 Collaboration, K.Abe et al., Phys.Rev.Lett. 79 (1997) 26

[8] E143 Collaboration, K.Abe et al., Phys.Lett. B364 (1995) 61

[9] SMC Collaboration, D.Adams et al., Phys.Lett. B369 (1997) 338

[10] HERMES Collaboration, A.Airapetian et al., Phys.Lett. B442 (1998) 484

[11] HERMES Collaboration, K.Akerstaff et al., Phys.Lett. B444 (1998) 531

[12] SMC Collaboration, D.Adeva et al., Phys.Lett. B420 (1998) 180

[13] J.Collins, Nucl.Phys. B396 (1993) 161

[14] NMC Collaboration, M.Arneodo et al., Phys.Rev. D50 (1994) 1

[15] HERMES Collaboration, K.Akerstaff et al., Phys.Rev.Lett. 25 (1998) 5519

[16] E866 Collaboration, E.A.Hawker et al., Phys.Rev.Lett. 80 (1998) 3715

[17] HERMES Collaboration, K.Akerstaff et al., hep-ex/9811011